ScienceDirect
www.sciencedirect.com

Revista Iberoamericana de Automatica e Informática industrial (2023) 1–5

RIAI
www.elsevier.es/RIAI

Crystallographic Study of Materials with Grain Boundaries using Gabor Filters and K-means Clustering Methods

Andrei Hernandez-Robles[1], Brian A. Paniagua[1], Arturo Ponce[1]

Abstract

For the crystallographic study of materials with grain boundaries, this project examines the employment of Gabor filters and K-means clustering methods. We are concerned whether Gabor filters can successfully extract crystallographic data from Transmission Electron Microscopic (TEM) images of materials and whether this data can then be used by K-means clustering to categorize defects and produce crystal orientation maps. The use of K-means clustering and Gabor filters in combination with TEM images of materials with grain boundaries is thought to be an efficient tool for crystallographic investigation. Gabor filters, which are frequency-based filters capable of detecting sudden changes in intensity, such as grain boundaries, are used in the project for feature extraction. The K-means algorithm, an unsupervised learning technique, is then used to analyze the retrieved features in order to find patterns in the data. The research is significant because it offers a potential answer to the problem of evaluating TEM pictures of materials with grain boundaries, improving our understanding of their crystallographic structure, and providing information about the characteristics and performance of these materials. The technique's potential for automated grain boundary classification and crystal orientation mapping was shown by testing it on TEM images. The findings indicate that this approach is capable of detecting faults and extracting significant crystallographic information, making it a valuable tool for future materials research.

1. Introduction

Over the past few decades, there has been extensive research on nanocrystalline materials, and, particularly in the last few years, there has been considerable development in our understanding of these materials (1). Nanocrystalline materials are single or multi-phase polycrystals with nanoscale grains, which may significantly alter their physical, mechanical, and chemical properties in comparison with conventional coarse-grained polycrystalline materials (2). Traditionally, atomic resolution images of materials have been obtained using transmission electron microscopy (TEM) techniques. Techniques like electron diffraction have also been applied to materials to display crystallographic data (3). Computational tools, such as particle segmentation algorithms based on supervised and unsupervised learning techniques, have been developed to study the crystallographic profile of nanomaterials (4). Tracing the particle form and size and crystal orientation mapping are the two basic divisions of these approaches. Computer vision-based techniques can be used for electron microscopy analysis to avoid the collecting and processing of enormous quantities of data to train these models, even if learning-based approaches require extensive training datasets with precise parameters (4).

Grain boundaries in polycrystalline materials are contacts between two grains or crystallites (5). These two dimensional flaws in the crystal structure play an important role in defining a material's qualities. Grain boundaries lower the material's electrical and thermal conductivity, making them a favored site for the initiation of corrosion and the precipitation of new phases from the solid (5). The significance of grain boundaries is further demonstrated by their effect on the electrical characteristics that regulate the system's varistor behavior. In ZnO, for example, an increase in grain boundary-mediated densification of more than an order of magnitude would be difficult to explain by a process other than grain boundary complexions (6). In materials science, grains or crystallites are microscopic crystals that develop during the cooling (crystallization) of various materials. A metal's average grain size is an important characteristic. The mechanical characteristics of a material are directly affected by grain size. Smaller grains, for example, have better strength and hardness, but bigger grains have higher ductility and toughness (7).

The research that will be presented here combines a particle segmentation technique based on Gabor filters with atomic scale crystal orientation mapping to analyze metallic nanoparticles grain boundaries. This technique is significant due to it not only for it's ability to demonstrate the accuracy of crystal segmentation at individual nanoparticle scales, but also offers the opportunity to expand the application into a dynamic analysis of particle transformation captured with aberration-corrected mi-

croscopy (8). This opens new possibilities for nanoscale analysis, thereby enhancing the scope and utility of the method. Overall, this research advances our knowledge of nanomaterials and their properties and offers a fresh method for examining the crystallographic profile of nanomaterials without the use of experimental methods or model-based learning.

2. Methods

2.1. Gabor Filters

Renowned British-Hungarian physicist Dennis Gabor made significant contributions to the fields of optics and microscopy. Gabor's research on electron microscopy led to his invention of the holography technique, a method for creating three-dimensional images of small objects using the principles of interference and diffraction (9). Gabor received the 1971 Nobel Prize in Physics for his ground-breaking work. The development of holography created new opportunities for the study of microscopic structures and had a profound impact on a number of disciplines. Researchers studying the structure of molecules can utilize holography to produce incredibly accurate, three-dimensional photographs of particles (9). Fiber optic communication systems were created as a result of Gabor's contributions to communication theory. Furthermore, his research on microscopy led to the development of Gabor filters in 1946 as a way to describe the structure of the human visual system (10).

Also known as a Gabor wavelet or a Gabor kernel, gabor filters is a mathematical function used in image processing and computer vision to analyze and manipulate images (10). They are based on the uncertainty principle between a signal's inability to be simultaneously localized in both frequency and time domains (8). Gabor showed that the most general function to attain a minimum of the uncertainty principle, which therefore, delivering the greatest accuracy in the time-frequency scale combined space, is the product of a Gaussian-shaped kernel times a complex sinusoid (8) (11). The two dimensional model of the Gabor filter has particularly shown its utility in texture analysis, feature extraction, edge detection and a plethora of image related fields. This is due to the fact that the Gabor filter is made up of a Gaussian and a sinusoid and so its Fourier transform is the convolution of these transforms (8). This property allows Gabor filters to efficiently extract features based on their fringe orientation and spacing, making them useful for analyzing electron microscopy images of crystalline materials.

In the spacial domain, a 2D Gabor filter is defined as a sinusoidal plane wave modulated by a Gaussian envelope. It can be mathematically expressed as:

$$g(x, y; \sigma_x, \sigma_y, \theta, \gamma, \lambda, \phi) = e^{\frac{-1}{2}\left(\frac{x'^2}{\sigma_x^2} + \frac{y'^2\gamma^2}{\sigma_y^2}\right)} e^{i\left(2\pi\frac{x'}{\lambda} + \phi\right)}$$

where this equation contains two parts multiplied together: the Gaussian shape kernel (the envelope) w and the complex sinusoid (the carrier) s.

$$w(x, y) = \frac{1}{\sqrt{2\pi\sigma}} e^{\frac{-1}{2}\left(\frac{x'^2}{\sigma_x^2} + \frac{y'^2\gamma^2}{\sigma_y^2}\right)}$$

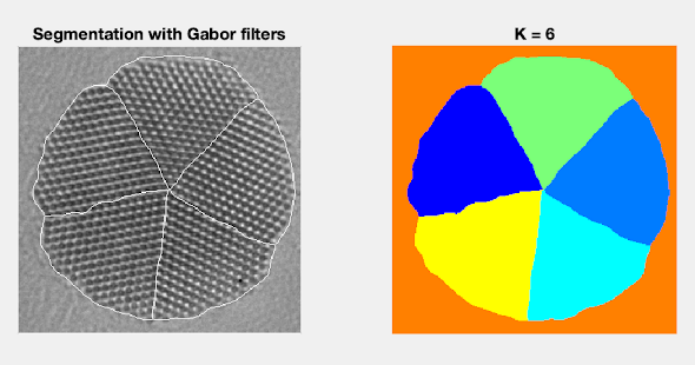

Figure 1: Particle segmentation of a HRTEM decahedral nanoparticle at k=6 (Left) and colorization of the segmentation (right) to visualize the overall morphology of the structure.

and

$$s(x, y) = e^{-2\pi i(u_0 x + v_0 y + \psi)}$$

where,

$$x' = x\cos\theta + y\sin\theta$$

$$y' = -x\sin\theta + y\cos\theta$$

where σ_x^2 and σ_y^2 are the coordinates of a point in the image and determines the size of the major and minor axis of the Gaussian envelope, and u_0 and v_0 are the parameters that govern the spacial frequency of the sinusoid and ψ is the phase (8).

The important parameters of the Gabor filter are the wavelength λ, which determines the spatial frequency of the sinusoidal wave, also can be referred to as the filtering channel (8). The orientation θ, which controls the direction of the filter's response, the phase offset ϕ, which shifts the center of the filter's response, the standard deviation σ, which determines the size of the Gaussian envelope, and the aspect ratio γ, which controls the shape of the Gaussian envelope (12). By varying these parameters, different Gabor filters can be created to extract different features from an image.

Gabor filtering can highlight local textures based on their orientation and wavelength. This is done by an image $f(x, y)$ multiplied by the Gabor filter $g(x, y; \sigma_x, \sigma_y, \theta, \gamma, \lambda, \phi)$. These parameters can be changed to accentuate textures with various fringe patterns. The filter bandwidth, which defines which portion of the image contributes to a given pixel value, and can be adjusted using the (σ_x, σ_y) parameters (8). A collection of Gabor filters with various orientations and spacings can be created and used to characterize each pixel based on the surrounding fringe patterns in order to extract pertinent characteristics from an image (8).

To utilize Gabor filters for image feature extraction, a bank of filters with distinct orientations and spatial frequencies is often developed. Each filter is convolved with the input picture to generate a response image that emphasizes portions of the image that are most similar to the frequency and orientation of the filter (13). The response photos are then merged to form a feature map, which depicts the distribution of relevant characteristics in the original image.

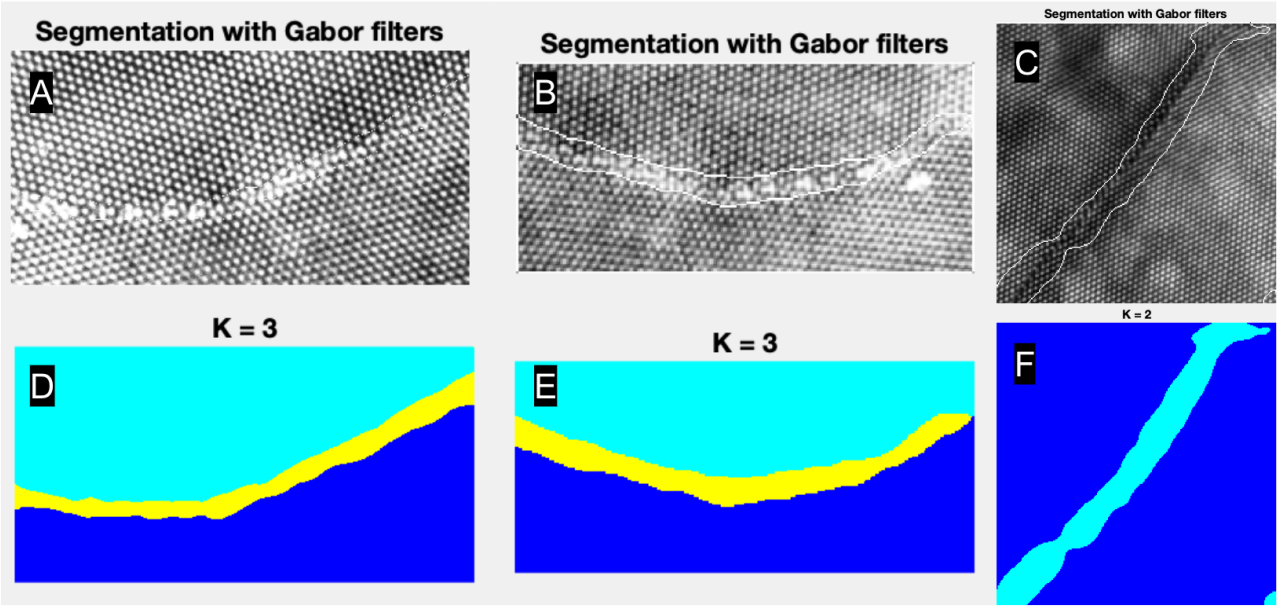

Figure 2: Three cross sections of ZnO, containing Σ = 13 grain boundaries at various angles, A) Segmentation on a cross section at K=3, B) Segmentation on a cross section at K=3, C) Segmentation on a cross section at K=2, (D) Colorization of the segmentation done in (A), E) Colorization of the segmentation done in (B), F) Colorization of the segmentation done in (C)

2.2. *K-Means Clustering*

Unsupervised learning is a type of machine learning in which the algorithm picks up on structures and patterns in the data without any direct supervision or direction from labeled examples (14). In other words, the algorithm looks for underlying patterns, groupings, or relationships within the data rather than being given specific outputs to forecast or classify. This makes it practical for locating hidden patterns or structures in large, complicated datasets when manually labeling the data may be challenging or time-consuming. Unsupervised learning methods come in a variety of forms, including clustering, dimensionality reduction, and anomaly detection (14). In clustering, more specifically, in K-means clustering data points are grouped into K clusters based on their distance from each group's centroid. The data points that are clustered together are those that are closest to a centroid. The K value determines the number of clusters in direction proportionality, where a larger K value indicates smaller groupings and more granularity, and a smaller K indicates larger groupings and less granularity (14). Market segmentation, document and picture grouping, and image compression all use K-means clustering algorithms.

2.3. *Feature Extraction*

To properly map the crystal orientation of nanoparticles in HRTEM images of grain boundaries, this study employs Gabor filters for feature extraction and unsupervised learning in image segmentation. Designing Gabor filters with certain orientations and wavelengths associated with distinct reflections and applying them to the entire picture is the approach. The resultant response picture emphasizes the pixels that correspond to the same region, enabling for exact mapping of the crystal orientation of the nanoparticles (15). The findings of this study show that Gabor filters are effective in mapping the crystal orientation of nanoparticles in HRTEM images of grain boundaries. The technology provides a very precise and accurate method for crystal orientation mapping and may be used in a variety of materials science applications (16). Figure 1 shows an example of feature extraction to determine a decahedral nanoparticle's facets. This particle was collected using HRTEM using 200 kV. At K=6, the segmentation method correctly detected the predicted five facets of the decahedral nanoparticle as well as the background. The algorithm was able to detect the expected five facets and the background at K=6. It is worth mentioning that the segmentation process converged at K=n+1, where n is the particle's number of facets.

3. Results

Figure 2 depicts the segmentation of a ZnO cross section containing a Σ = 13 grain boundary at particular angles. In Figure 2A,D shows cuts of a grain boundary in the horizontal direction where the segmentation occurred for K=3; two for each side of the crystal and one for the grain boundary interface. By following the steps outlined above the segmentation was successful at detecting each crystal and the interface. Figure 2C is a cut of a grain boundary positioned at 45°. For this instance, the segmentation occurred for K=2 and recognized the crystal background along with the grain boundary interface. There does exist some noise within the image but it is negligible and did not significantly affect the accuracy of the segmentation. To provide a more comprehensive understanding of the segmentation results, Color maps of the segmentation of the 3 cuts of ZnO are shown in Figure 2D,E,F in their respective order. These color maps give a visual representation of the various

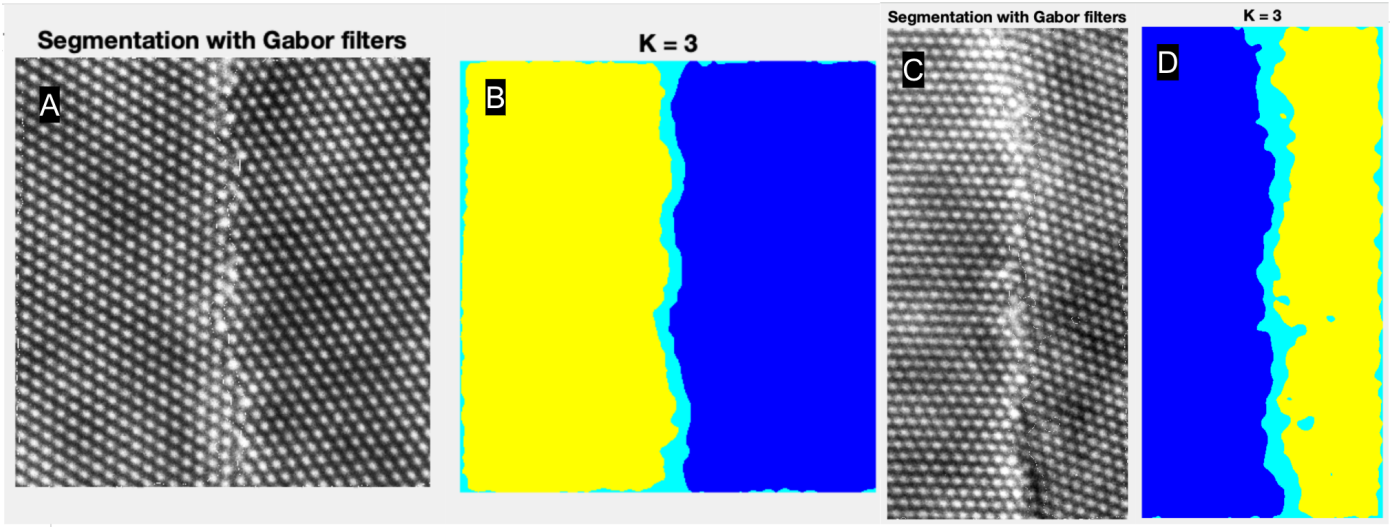

Figure 3: Two cross sections of ZnO, A) Segmentation at K=3 of a $\Sigma = 7$ grain boundary, B) Colorization of the segmentation done in (A), C) Segmentation at K=3 of a $\Sigma = 31$ grain boundary, D) Colorization of the segmentation done in (C)

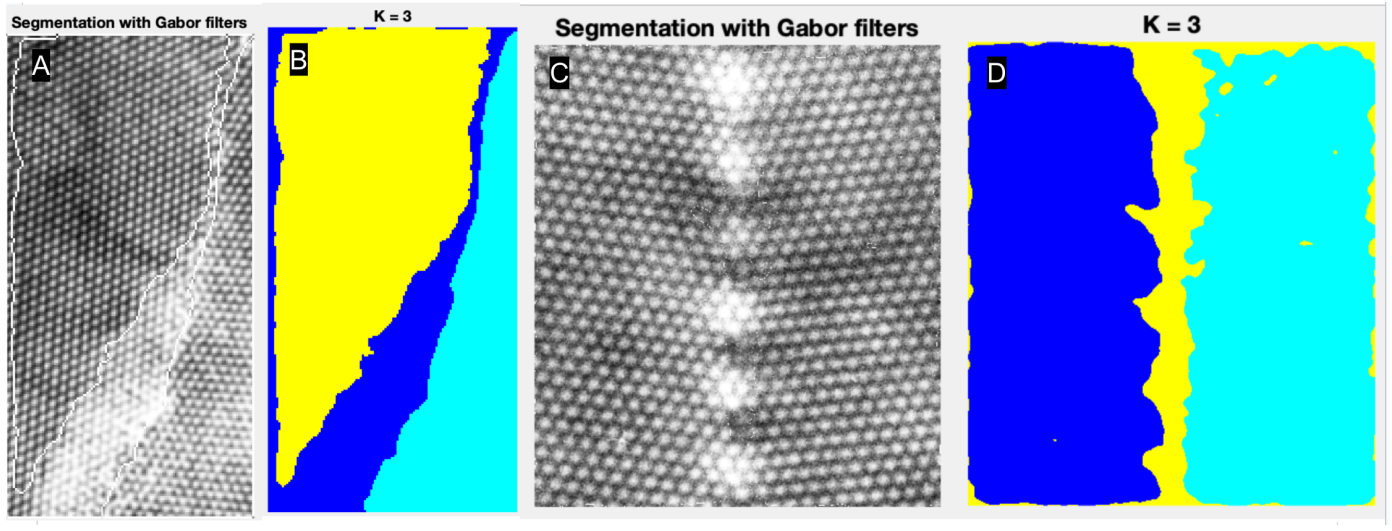

Figure 4: Two cross sections of ZnO, A) Segmentation at K=3 of a $\Sigma = 13$ grain boundary, B) Colorization of the segmentation done in (A), C) Segmentation at K=3 of a $\Sigma = 19$ grain boundary, D) Colorization of the segmentation done in (C)

segments detected by the algorithm and may be used to further evaluate the grain boundary features.

Figure 3 depicts the study of a cross-section of ZnO with a $\Sigma = 7$ grain boundary and a $\Sigma = 31$ grain boundary. Figure 3 shows images that were cut in such a way that the grain boundary is vertical for segmentation. It is worth noting that the segmentation analysis for both cuts detected three locations in K=3: the two ZnO crystal facets and the grain boundary interface, which is consistent with Figure 2D,E results. This observation is especially significant since it implies that grain boundary segmentation happens in the majority of situations where K=3. Furthermore, while there were some instances of noise in the findings for both segmentations, the algorithm was able to optimally distinguish the grain boundary interface existing within the particle.

The images in the next set show a cross-section of ZnO with a $\Sigma = 13$ (Figure 4A,B) grain boundary and a $\Sigma = 19$ (Figure 4C,D) grain boundary. These photos are especially of interest because they illustrate how the segmentation process may efficiently follow rough spots inside the crystal's grains as well as any anomalies in the particle. This is a significant discovery since it illustrates the segmentation algorithm's resilience in dealing with complicated microstructures. Interestingly, the segmentation results for both slices of the ZnO particle fall for K=3, which is consistent with prior images' segmentation results. This consistency in the findings underscores the segmentation algorithm's efficacy and dependability in recognizing grain boundaries and crystal facets in ZnO particles.

In the final set of photos, Figure 5A-F, we see two more cross-sections of ZnO particles with a $\Sigma = 13$ grain boundary, but with three crystals instead of the two as previously shown. These photos give more insight into the segmentation

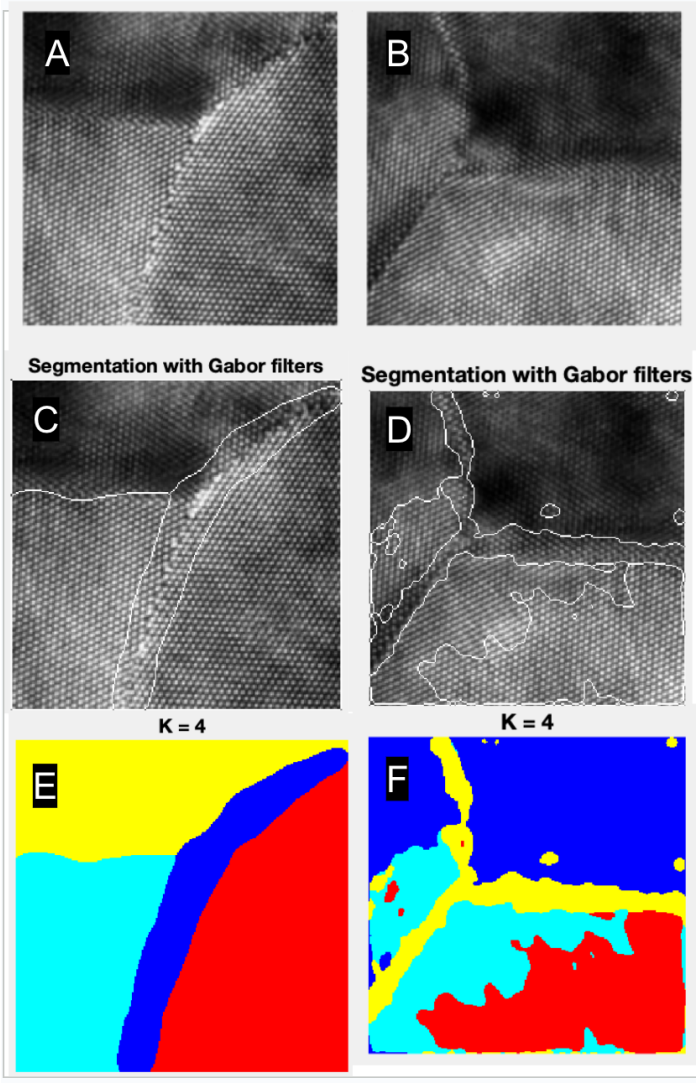

Figure 5: Two cross sections of ZnO containing Σ = 13 grain boundaries with three crystals, A) Without segmentation of a cut of ZnO with three crystals, B) Without segmentation of a different cut of ZnO with three crystals, C) Segmentation of (A) at K=4, D) Segmentation of (B) at K=4, E) Colorization of the segmentation done in (C), F) Colorization the segmentation done in (D)

algorithm's behavior while dealing with complicated microstructures. Interestingly, both cuts of the ZnO particle were segmented at K=4, which differs from earlier results. The segmentation correctly detected each crystal, as well as the grain boundary interface and the grain border, in Figures 5A, C, and E. The program was able to efficiently segment the particle and identify the important characteristics present, which can assist in the understanding of ZnO particle microstructure. The segmentation analysis in Figures 5B, D, and F was performed at K=4. Despite the fact that the segmentation procedure detected several abnormalities within the particle, the system correctly identified the grain boundary interface. This discovery emphasizes the segmentation algorithm's stability and ability to reliably detect essential elements in complicated microstructures.

4. Conclusion

Here we review a method for segmentation of crystalline nanoparticles based on the use of a bank of Gabor filters as a feature extraction technique and an unsupervised learning strategy, K-means clustering, for particle segmentation. The method can segment numerous particles and determine crystal orientation, allowing for the development of atomic-resolution maps. However, one shortcoming of the technique is that it necessitates fine-tuning the initial parameters for each image, which can be a time-consuming operation. To circumvent this issue, it would be good to have a method to automatically calculate the initial parameters. A solution is to use a more advanced deep learning techniques which could be used for more complicated tasks in the future. These strategies have the ability to automate the parameter optimization process and result in more accurate outcomes. Overall, the suggested methodology makes an important contribution to the field of crystalline nanoparticle segmentation and has the potential to be further refined and optimized in the future.

References

[1] H. Gleiter, B. Chalmers, Progress in mater, Sci 33 (1989) 223.
[2] M. Meyers, A. Mishra, D. Benson, Mechanical properties of nanocrystalline materials, Progress in Materials Science 51 (4) (2006) 427–556.
[3] C. Ophus, Four-dimensional scanning transmission electron microscopy (4d-stem): From scanning nanodiffraction to ptychography and beyond, Microscopy and Microanalysis 25 (3) (2019) 563–582.
[4] C. K. Groschner, C. Choi, M. C. Scott, Machine Learning Pipeline for Segmentation and Defect Identification from High-Resolution Transmission Electron Microscopy Data, Microscopy and Microanalysis 27 (3) (2021) 549–556.
[5] E. Lehockey, G. Palumbo, P. Lin, A. Brennenstuhl, On the relationship between grain boundary character distribution and intergranular corrosion, Scripta Materialia 36 (10) (1997) 1211–1218.
[6] S. J. Dillon, K. Tai, S. Chen, The importance of grain boundary complexions in affecting physical properties of polycrystals, Current Opinion in Solid State and Materials Science 20 (5) (2016) 324–335.
[7] (USDOE), Doe fundamentals handbook: Material science. volume 1 (1 1993).
[8] G. Bárcena-González, A. Hernández-Robles, Á. Mayoral, L. Martinez, Y. Huttel, P. L. Galindo, A. Ponce, Unsupervised learning for the segmentation of small crystalline particles at the atomic level, Crystal Research and Technology (2022) 2200211.
[9] Ethw, Milestones:invention of holography, 1947 (Jun 2022).
[10] J. G. Daugman, Uncertainty relation for resolution in space, spatial frequency, and orientation optimized by two-dimensional visual cortical filters, J. Opt. Soc. Am. A 2 (7) (1985) 1160–1169.
[11] A. K. Jain, F. Farrokhnia, Unsupervised texture segmentation using gabor filters, Pattern recognition 24 (12) (1991) 1167–1186.
[12] I. Fogel, D. Sagi, Gabor filters as texture discriminator, Biological cybernetics 61 (2) (1989) 103–113.
[13] J.-K. Kamarainen, V. Kyrki, H. Kalviainen, Invariance properties of gabor filter-based features-overview and applications, IEEE Transactions on image processing 15 (5) (2006) 1088–1099.
[14] J. Delua, Supervised vs. unsupervised learning: What's the difference? (Mar 2021).
[15] X. Wang, X. Ding, C. Liu, Gabor filters-based feature extraction for character recognition, Pattern Recognition 38 (3) (2005) 369–379.
[16] W. Li, K. Mao, H. Zhang, T. Chai, Selection of gabor filters for improved texture feature extraction, in: 2010 IEEE International Conference on Image Processing, 2010, pp. 361–364.